

NO-A191 549

NOVEL FIBER PREFORMS: RARE EARTH DOPING(U) BROWN UNIV  
PROVIDENCE RI DIV OF ENGINEERING T F MORSE 21 JAN 88  
AFOSR-TR-88-0221 AFOSR-87-0050

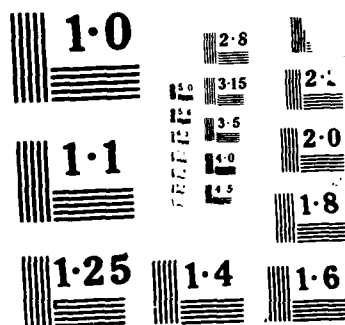
1/1

UNCLASSIFIED

F/G 7/2

ML





DTIC FILE COPY

AFOSR-TR- 88-0058

2

AD-A191 549

NOVEL FIBER PREFORMS: RARE EARTH DOPING

T. F. Morse  
Division of Engineering  
Brown University  
Providence, Rhode Island 02912

DTIC  
ELECTE  
MAR 02 1988  
S D  
C2D

January 21, 1988

Final Technical Report for the period: November 1, 1986 to November 30, 1987

AFOSR-87-0058

Air Force Office of Scientific Research  
Bolling Air Force Base  
Washington, D.C. 20332

Endorsements:

T. F. Morse  
T. F. Morse  
Professor of Engineering

Carl Cometta  
Mr. Carl Cometta  
Executive Officer  
Division of Engineering

88 2 28 128

## REPORT DOCUMENTATION PAGE

1a. REPORT SECURITY CLASSIFICATION None, <i>Unclassified</i>			1b. RESTRICTIVE MARKINGS None	
2a. SECURITY CLASSIFICATION AUTHORITY None			3. DISTRIBUTION/AVAILABILITY OF REPORT Unrestricted	
2b. DECLASSIFICATION/DOWNGRADING SCHEDULE N/A				
4. PERFORMING ORGANIZATION REPORT NUMBER(S) None			5. MONITORING ORGANIZATION REPORT NUMBER(S) <b>AFOSR-TK- 88-0221</b>	
6a. NAME OF PERFORMING ORGANIZATION Brown University		6b. OFFICE SYMBOL (If applicable) N/A	7a. NAME OF MONITORING ORGANIZATION AFOSR	
6c. ADDRESS (City, State and ZIP Code) Division of Engineering Box D Providence, RI 02912			7b. ADDRESS (City, State and ZIP Code) Bolling Air Force Base Washington, DC 20332-6448	
8a. NAME OF FUNDING/SPONSORING ORGANIZATION AFOSR		8b. OFFICE SYMBOL (If applicable) N/A	9. PROCUREMENT INSTRUMENT IDENTIFICATION NUMBER AFOSR-87-0058	
8c. ADDRESS (City, State and ZIP Code) <i>Same as 7b</i>			10. SOURCE OF FUNDING NOS.	
			PROGRAM ELEMENT NO. <i>61102F</i>	TASK NO. <i>2305/102</i>
11. TITLE (Include Security Classification) <i>Novel Fiber Preforms: Rare Earth Doping</i>			WORK UNIT NO. <i>B2</i>	
12. PERSONAL AUTHOR(S) T. F. Morse, Professor of Engineering				
13a. TYPE OF REPORT Final Technical Report		13b. TIME COVERED FROM <i>11/1/86</i> TO <i>11/30/87</i>	14. DATE OF REPORT (Yr., Mo., Day) 88/1/21	
15. PAGE COUNT 17 plus 2 Encls.				
16. SUPPLEMENTARY NOTATION				
17. COSATI CODES			18. SUBJECT TERMS (Continue on reverse if necessary and identify by block number)	
FIELD	GROUP	SUB. GR.	Optical fiber preform, Fiber sensor, Frequency doubling, Rare earth doping	
19. ABSTRACT (Continue on reverse if necessary and identify by block number)				
<p>Rare earth glasses have been studied with emphasis on those characteristics related to rare earth doping of optical fiber preforms for fiber sensor applications.</p>				
20. DISTRIBUTION/AVAILABILITY OF ABSTRACT UNCLASSIFIED/UNLIMITED <input checked="" type="checkbox"/> SAME AS RPT. <input type="checkbox"/> DTIC USERS <input type="checkbox"/>			21. ABSTRACT SECURITY CLASSIFICATION None	
22a. NAME OF RESPONSIBLE INDIVIDUAL <i>T. F. Morse</i>			22b. TELEPHONE NUMBER (Include Area Code) <i>(401) 863-1111</i>	22c. OFFICE SYMBOL <i>NE</i>

**October 31, 1986-November 1, 1987**

Division of Engineering

Department of Chemistry, Brown University, Providence, R.I. 02912

In conjunction with our research of novel dopants in optical fibers, we have initiated a program of cooperative research with Major J. Rotger, Frank J. Seiler U.S. Air Force Research Laboratory, Colorado Springs, and with Dr. Ulf Osterberg, a member of Prof. Stegeman's group at the University of Arizona, Optical Science Center. Dr. Osterberg, whom I recently visited, is carrying on some of his second harmonic experiments with phosphorus doped silica based fibers supplied by our laboratory. Dr. Osterberg is also setting up some experiments in conjunction with Major Rotger in the area of frequency doubling, and fibers from our facility are being used in this effort. The goal will be to



A-1

increase the efficiency of this process, and to understand the basic mechanism responsible for this unexpected phenomenon. To this latter end, we have already obtained NMR spectra of our phosphorus doped fibers, and hope to obtain sufficient lengths of Nd:YAG irradiated fibers from Dr. Osterberg at the University of Arizona to use in Prof. Bray's (Department of Physics, Brown University) NMR facility. This may provide some insight into the details of the mechanism responsible for the breaking of the symmetry that permits second order harmonic generation in an amorphous glass. The fiber group at the University of Southampton, Southampton, England, has recently obtained 10% efficiency in their frequency doubling experiments.

We are also continuing our efforts in rare earth doped glasses, with the ultimate use as fiber lasers or fiber sensors. The glass-science aspect of our efforts in this area has been carried out in the laboratory of Prof. Risen, of the Department of Chemistry. Dr. Kang Sun recently completed his Ph.D. degree in the area of rare earth glasses, and recent publications associated with this work are attached.

In summary, progress has been made in the following areas: further experience with ~~out~~ (MCVD) preform facility, and the establishment of ~~an~~ <sup>an</sup> optical draw tower provides ~~us~~ <sup>the</sup> with ~~with an~~ ability to create state-of-the-art fibers with a host of novel dopants. We will continue to concentrate on fibers doped with rare earth elements by several techniques, and to continue studies of bulk formation of rare earth glasses, with Prof. W. Risen, Jr. (Chemistry Department) and to study certain aspects of second harmonic generation in rare earth doped silica based fibers. This work will be undertaken in conjunction with Dr. Osterberg in Prof. Stegeman's group at the University of Arizona, and Major Rotger's group at Colorado Springs.

*Robert C. Evers*



## RARE EARTH PHOSPHATE GLASSES

Kang Sun and William M. Risen, Jr.  
Department of Chemistry, Brown University, Providence, RI 02912, U.S.A.

(Received 4 September 1986 by J. Tauc)

Praseodymium phosphate and dysprosium phosphate glasses with compositions  $x\text{Ln}_2\text{O}_3(1-x)\text{P}_2\text{O}_5$  have been synthesized and analyzed to be in the  $x=0.18-0.30$  range. Their structures have been studied by infrared, far infrared and laser Raman spectroscopy, and the dependences of the magnetic and thermal properties of the glasses on stoichiometry and structure have been investigated.

### Introduction

The characteristics of glasses containing high concentrations of rare earth ions are of considerable interest for applications in optical data transmission, detection, sensing, and laser technologies. Such glasses can have high magnetic susceptibilities and strong, sharp electronic absorptions in the ultraviolet to near infrared region, and thus may be useful as Faraday rotator modulators, optical isolators, fiber lasers, and optical signal couplers.

While there are many complex multicomponent rare earth glasses, phosphates hold special interest as binary rare earth glasses of variable composition whose properties can be changed systematically. Segal and coworkers<sup>1,2</sup> have reported the magneto-optic properties of one composition of each of the rare earth phosphates, but to gain control over such materials it is important to determine how the spectral, magnetic and thermal characteristics vary with composition. We report the synthesis, analysis and key features of the laser Raman and infrared spectra, the glass transition behavior and the magnetic susceptibilities of the binary glasses  $x\text{Pr}_2\text{O}_3(1-x)\text{P}_2\text{O}_5$  and  $x\text{Dy}_2\text{O}_3(1-x)\text{P}_2\text{O}_5$ , with  $x$  in the 0.18 to 0.30 range. These lanthanide elements, Pr and Dy, were chosen in order to include both large and small valence-stable rare earth ions, since cation size is an important determinant of the glass forming regions of rare earth glasses, and to include ions with both high and low free ion magnetic susceptibilities,  $\chi$ , since the Verdet constant depends strongly on  $\chi$ .

### Experimental

Glasses with compositions  $x\text{Pr}_2\text{O}_3(1-x)\text{P}_2\text{O}_5$  ( $x=0.18-0.28$ ) and  $x\text{Dy}_2\text{O}_3(1-x)\text{P}_2\text{O}_5$  ( $x=0.24-0.29$ ) have been obtained from 99.9%  $\text{Pr}_2(\text{CO}_3)_3$ , 99.99%  $\text{Dy}_2(\text{CO}_3)_3$  and 99.9%  $\text{P}_2\text{O}_5$  by quenching in air melts of mixtures of  $\text{Ln}_2(\text{CO}_3)_3$  and  $\text{P}_2\text{O}_5$  that were heated in covered Pt crucibles at  $1400^\circ\text{C}$  for one hour. A wide range of ratios of amounts of starting materials were used in attempts to prepare glasses outside of the  $x=0.2-0.3$  composition range, but the only resultant homogeneous vitreous materials formed by this method fell in that range. All reported materials were examined by x-ray diffraction.

The elemental compositions were determined to within  $\pm 0.01$  weight percent by electron microprobe analysis. The

microprobe data were measured with a Cameca Microprobe using a 15kV - 10nA beam at a  $40^\circ$  take off angle. The glass transition temperatures,  $T_g$ , were measured under  $\text{N}_2$  on a DuPont 9900 DTA/DSC thermal analyzer on annealed samples in Pt cells with  $\text{Al}_2\text{O}_3$  as the reference. Magnetic susceptibilities were measured at  $25^\circ\text{C}$  on a Faraday balance with a field strength of 10.40kOe and field gradient,  $H(dH/dz)$ , of 17.93. Raman spectra were measured on a Spex 1403 spectrometer with 514.5nm Ar ion laser radiation using the  $90^\circ$  scattering geometry. Infrared measurements were made on a Digilab FTS-15B as KBr pellets from  $3800-400\text{cm}^{-1}$  and as low density polyethylene pellets ( $50-500\text{cm}^{-1}$ ). Spectral resolution was  $2\text{cm}^{-1}$  or better in all cases.

### Results and Discussion

The microprobe analyses of the glasses formed showed them to have the compositions listed in Table 1. Since the analysis of 40 randomly selected  $0.15\mu$  regions on each glass gave identical results and x-ray diffraction and Raman spectra gave no evidence of crystallinity, these materials are amorphous and are homogeneous with no possible phase separation at a level greater than about  $0.07\mu$ .

The range of compositions, approximately  $x=0.2$  to  $x=0.3$  for  $x\text{Ln}_2\text{O}_3(1-x)\text{P}_2\text{O}_5$ , corresponds to glasses with P:O ratios of 0.348 to 0.318. At  $x=0.25$  this ratio is 0.333 and the glass has the metaphosphate composition. While there are several possible structural types at this composition,  $(\text{PO}_3)_n$  chains dominate in alkali metaphosphate glasses.<sup>3</sup> At values of  $x$  below 0.25, some of the ring and bridge structures of  $\text{P}_2\text{O}_7$  should be present along with  $(\text{PO}_3)_n$  chain segments in the network. When  $x$  exceeds 0.25, the phosphate portion of the network is expected to be composed of shorter chains and to approach the  $\text{P}_4\text{O}_{13}^{4-}$  ion at  $x=0.33$ .

Thus, this composition region includes glasses whose network structures should range from partial ring-partial chain, to long chain, to short chain in character. The experimental questions, once the glass formation region is defined, are: whether these structural conjectures are supported by spectroscopic data; how they and the properties of the rare earth ions affect the glass transition; and, how the structure and composition are related to the magnetic properties of the glasses.

The Raman and infrared spectra of all glasses in these series were obtained, and those of three  $x\text{Pr}_2\text{O}_3(1-x)\text{P}_2\text{O}_5$  glasses, selected to represent the results over the range in  $x$ , are in Figures 1 and 2. The complete spectra and vibrational assignments will be reported elsewhere. The spectra exhibit major variations as a function of rare earth concentration,  $x$ , over the  $x=0.202$  to  $x=0.284$  range. These are evident in the 1200–1400, 850–1150 and 600–800  $\text{cm}^{-1}$ , as well as lower frequency regions of the Raman spectra in Figure 1. For comparison, the  $x=0.202$  spectrum is repeated as a dashed line without offset relative to that of  $x=0.234$ .

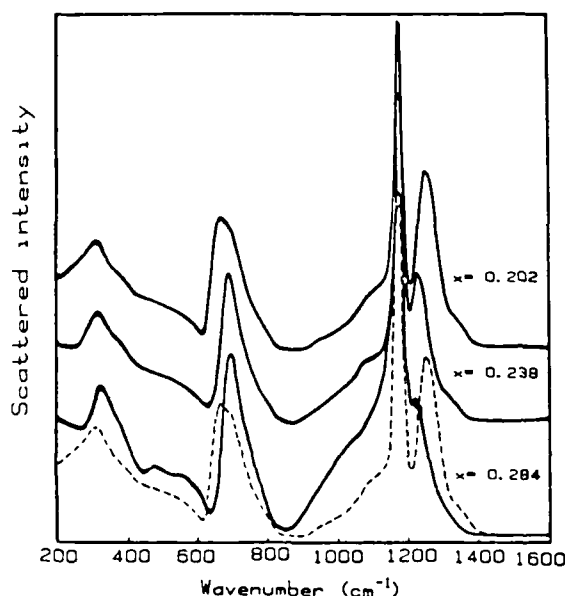


Figure 1. Raman spectra of  $x\text{Pr}_2\text{O}_3(1-x)\text{P}_2\text{O}_5$  glasses at  $x$  values noted for solid lines. The dashed line repeats the  $x=0.202$  spectrum without offset.

The change in frequency and relative intensity of the band maximum at  $1265\text{ cm}^{-1}$  to a shoulder at  $1220\text{ cm}^{-1}$  with a change in  $x$  of 0.082 is quite dramatic. It and analogous results for Dy-based glasses reveal changes that are great enough to serve as an analytical probe to determine the composition of rare earth phosphate glasses to an accuracy of at least  $\pm 0.01$  in  $x$ . Band contour analysis shows that this feature is not due to one band shifting but to the change in relative intensity of two bands, at ca  $1285$  and  $1220\text{ cm}^{-1}$ , whose convoluted band maximum shifts. These bands are due to the asymmetric  $\text{PO}_2$  stretch of  $\text{PO}_3$  units in the chain but different bonding configurations relative to the rare earth ions. As  $x$  increases a shoulder at ca  $1350\text{ cm}^{-1}$ , due to stretches of uncoordinated  $\text{P}=\text{O}$  units, disappears, and the strongest band, due to the  $\text{PO}_3$  symmetric stretch broadens and shifts from  $1188\text{ cm}^{-1}$  to lower frequency. In Dy-based glasses, containing the smaller but identically charged  $\text{Dy}^{3+}$  ion, this band is at  $1198\text{ cm}^{-1}$  at low  $x$  and decreases analogously. Part of the broadening of the  $1188\text{ cm}^{-1}$  peak is due to the increase in the  $1220\text{ cm}^{-1}$  band, but a major part is due to the dramatic increase in scattered intensity in the 850–1150  $\text{cm}^{-1}$  region. This is assigned to vibrations of  $\text{PO}_2$  end groups, whose concentration increases as the phosphate chain length increases with increasing  $x$ .

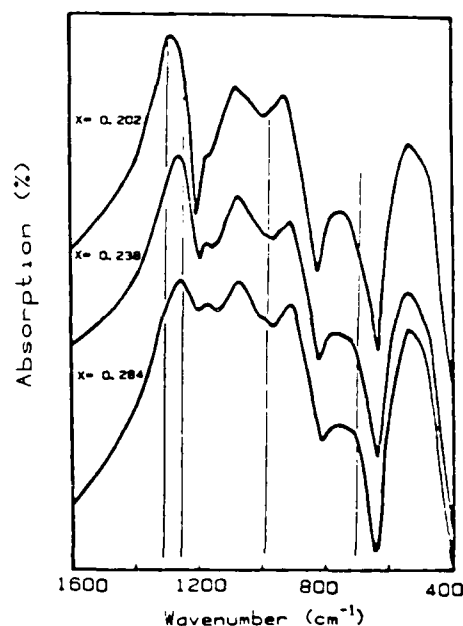


Figure 2. Infrared spectra of  $x\text{Pr}_2\text{O}_3(1-x)\text{P}_2\text{O}_5$  glasses, at  $x$  values noted, in the 400–1600  $\text{cm}^{-1}$  region.

These spectral changes are consistent with the structural hypotheses discussed above. The interpretation is supported further by the behavior of the lower frequency Raman bands and by the infrared spectra above  $400\text{ cm}^{-1}$ , which are shown in Figure 2. The Raman band at  $670\text{ cm}^{-1}$  in the  $x=0.202$  glass, is assigned to a predominately P–O–P stretching mode involving unperturbed chain and residual ring units in the  $\text{P}_2\text{O}_5$ -rich glasses. It appears at  $640\text{ cm}^{-1}$  in pure  $\text{P}_2\text{O}_5$  glass, in which there are no cation perturbations and the chain structure is not dominant, and above  $700\text{ cm}^{-1}$  in glasses near the metaphosphate composition. It decreases in intensity and is replaced by the band at ca  $715\text{ cm}^{-1}$  when  $x$  exceeds 0.238. Thus, the decrease of this band from one of the strongest in this spectrum to one of essentially zero intensity occurs with a change in  $x$  of as little as 0.036, and provides an excellent probe of stoichiometry and structure near the metaphosphate composition.

The infrared spectra above  $400\text{ cm}^{-1}$  contain a number of strong, extensively convoluted bands. While they reflect composition uniquely, most of the band shape changes are less dramatic than those in the Raman. However, the growth of the  $1170\text{ cm}^{-1}$  band, due to increased concentration of  $\text{PO}_2$  end groups as the phosphate chain becomes shorter when  $x$  increases, is evidenced by its change from a small shoulder at  $x=0.202$  to a strong band at  $x=0.284$ . Moreover, the shift of the strong  $\nu(\text{PO}_2)$  asymmetric stretching band structure from  $1280$  to  $1250\text{ cm}^{-1}$  is clear and consistent with the Raman analyses discussed above. Detailed band analysis reveals additional features, including the growth of  $980$  and  $720\text{ cm}^{-1}$  bands, which are consistent with these assignments. Overall, the vibrational spectra show that major structural changes occur in the  $x=0.2$  to  $0.3$  range. They are consistent with the network varying from partial ring-partial chain, to long chain, to short chain in character. Where comparable data are available for alkali and alkaline earth phosphates, and  $\text{P}_2\text{O}_5$ , these assignments also are consistent with the spectra.

**Table 1**  
Magnetic Susceptibilities of Rare Earth  
Phosphate Glasses

$x\text{Pr}_2\text{O}_3(1-x)\text{P}_2\text{O}_5$		$x\text{Dy}_2\text{O}_3(1-x)\text{P}_2\text{O}_5$	
$x$	$\chi \cdot 10^{-3}$ emu/mol	$x$	$\chi \cdot 10^{-2}$ emu/mol
0.188	1.90	0.240	2.33
0.202	1.98	0.262	2.54
0.216	2.13	0.277	2.62
0.222	2.25	0.289	2.76
0.238	2.36	0.298	2.83
0.284	2.86		

The values of the magnetic susceptibilities,  $\chi$ , given in Table 1 are in units of emu per mole of glass compound formulated as  $x\text{Ln}_2\text{O}_3 \cdot (1-x)\text{P}_2\text{O}_5$ , so the number of  $\text{Ln}^{3+}$  ions per mole increases with  $x$ . When these data are plotted it is seen that  $\chi$  varies nearly linearly with  $x$ . The slope of the best fit line which also includes  $\chi = 0$  (i.e.,  $\chi \leq 1 \times 10^{-5}$  for diamagnetic susceptibility) at  $x=0$  is  $0.950 \times 10^{-5}$  emu (mol glass) $^{-1}$  (mol  $\text{Ln}_2\text{O}_3$ ) $^{-1}$  for the Dy-containing glasses and  $1.01 \times 10^{-5}$  for those containing Pr. The only paramagnetic species present are the Ln ions, so their magnetic moments can be obtained from  $\chi$  using  $\mu_{\text{eff}} = 2.828 (\chi T)^{1/2}$  if the  $\chi$  values are normalized for composition. This gives  $\mu_{\text{eff}}(\text{Dy}) = 10.62$  BM and  $\mu_{\text{eff}}(\text{Pr}) = 3.46$  BM at 295K. These may be compared to the  $\mu_{\text{eff}}$

values expected from  $g[J(J+1)]^{1/2}$ , which are 10.64 BM for the  $^6\text{H}_{15/2}$  state of  $\text{Dy}^{3+}$  and 3.58 BM for the  $^3\text{H}_4$  state of  $\text{Pr}^{3+}$ . The linear variation of  $\chi$  with  $x$  and the comparison of calculated and observed values of  $\mu_{\text{eff}}$  show that neither the ligand field of the phosphate network nor any intercationic coupling is great enough to lift the  $(2J+1)$ -fold degeneracy of the ion states and that both are relatively small.

The glass transition temperatures, plotted in Figure 3, are found to vary linearly with  $x$  in each case and show two trends. First, Dy-containing glasses have higher  $T_g$ 's at each value of  $x$  than do the Pr glasses.<sup>2,3</sup> This is due

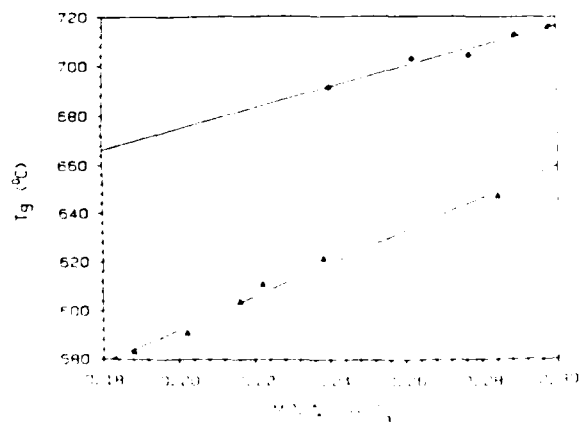


Figure 3. Glass transition temperatures of the rare earth phosphate glasses vs. composition. Mole %  $\text{Ln}_2\text{O}_3 = x$  in  $x\text{Ln}_2\text{O}_3 \cdot (1-x)\text{P}_2\text{O}_5$ . The upper curve is for Dy glasses and the lower curve for Pr glasses.

primarily to the fact that the smaller  $\text{Dy}^{3+}$  ion exerts a stronger electrostatic field on the network and increases the work required to overcome interionic forces and allow the network segments to rearrange at the glass transition.<sup>2</sup> Second, in both cases  $T_g$  increases with  $x$ . This is due to trade offs between several effects. As  $x$  increases above 0.25, the fraction of P atoms participating in terminal charged  $\text{PO}_3$  units increases and the chains become shorter. With the same variation, the ratio of  $\text{Ln}^{3+}$  to phosphate increases and the number of ionic crosslinking interactions per mole increases. Both the increase in the fraction of shorter, stiffer chains and the increase in strong ionic crosslinks serve to increase  $T_g$ . A smaller counteracting trend is a decrease in P-O-P crosslinking as  $x$  increases, but there are few ring- and crosslink-structures involving such bonds above  $x \approx 0.24$ , so their decrease is not a major effect.

The far infrared spectra of the glasses reflect the changes in the  $\text{M}^{3+}$ -network interaction as  $x$  is varied. As shown in Figure 4, the band structure due to vibrations of the cation relative to its neighboring phosphate network sites appears in the 150-275  $\text{cm}^{-1}$  region. In alkali metaphosphates this cation-motion band is at 102  $\text{cm}^{-1}$  for  $\text{CsPO}_3$ , for example, and increases to 212  $\text{cm}^{-1}$  for  $\text{NaPO}_3$ . In  $\text{M}^{3+}$  and  $\text{M}^{2+}$  metaphosphate series, generally, it decreases with cation mass and increases with cation charge.<sup>11</sup> Among metaphosphates with cations of similar mass but increased charge, the band increases in frequency from 102  $\text{cm}^{-1}$  for  $\text{Cs}^{+}$  (133 amu) to 116  $\text{cm}^{-1}$  for  $\text{Ba}^{2+}$  (137 amu) and, as shown in Figure 4, to 170-215  $\text{cm}^{-1}$  for  $\text{Pr}^{3+}$  (141 amu).

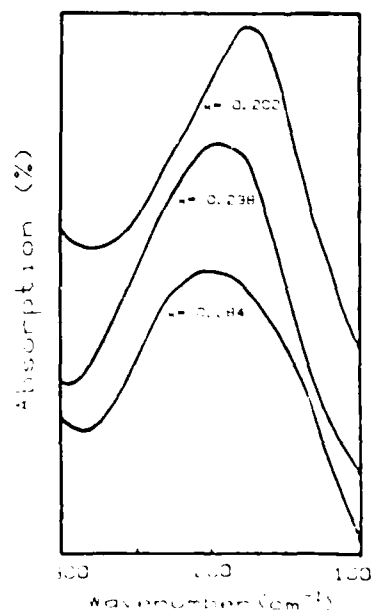


Figure 4. Far infrared spectra of  $x\text{Pr}_2\text{O}_3 \cdot (1-x)\text{P}_2\text{O}_5$  glasses in the 100-300  $\text{cm}^{-1}$  region at  $x$  values noted.

The composition dependencies of the cation-site band structures for the Pr and Dy glasses are complex and will be presented in detail later. But several observations are important to note. As  $x$  is increased the band shifts to higher wavenumbers, and the intensity increases, indicating stronger interaction of the cation with the phosphate network.

to cation-network stretches in which the network segments are  $\text{PO}_3$  units in  $(\text{PO}_3)_n$  chains and carry a net charge of -1, while those near  $220\text{ cm}^{-1}$  involve terminal  $\text{PO}_4$  units carrying a charge of -2. Clearly the cation-network forces reflected in the far infrared increase with  $x$ , as does  $T_g$ . The spectra of Dy glasses are similar to those of Pr glasses, although broadened to higher frequency. This is due to the fact that while Dy is some 24 amu heavier than Pr it is

smaller and has a higher charge to radius ratio.

Acknowledgement - We gratefully acknowledge the use of the MRL Facilities at Brown University, the assistance of Mr. Joseph Devine in obtaining the electron microprobe data, helpful discussions with Prof. Theodore Morse, and support of this work by the AFOSR under contract AFOSR-85-0304.

#### References

1. S. B. Berger and C. B. Rubinstein, J. Chem. Phys. **35**, 1978(1964).
2. S. B. Berger, C. B. Rubinstein, C. R. Kurkjan and A. W. Treptow, Phys. Rev. **133**, A723(1964).
3. Ya. S. Bobovich, Opt. Spectrosc. **13**, 492(1961)(Opt. Spectrosc. **13**, 274(1962).
4. G. J. Exarhos, P. J. Miller and W. M. Risen, Jr., J. Chem. Phys. **60**, 4145(1974).
5. G. Kh. Cherches, V. V. Pechkovskii, M. I. Kuz'menkov, and T. I. Barannikova, Fiz. Khl. Stek. **4**, 233(1978).
6. F. L. Galeener and J. C. Mikkelsen, Jr., Solid St. Commun. **30**, 505(1979).
7. G. J. Exarhos and W. M. Risen, Jr., Solid St. Commun. **11**, 755(1972).

## SOL-GEL PREPARATION OF RARE-EARTH SILICATE GLASSES

Kang SUN, Wook-Hwan LEE and William M. RISEN Jr

*Department of Chemistry, Brown University, Providence, RI 02912, USA*

Received 16 February 1987

Rare-earth silicate glasses have been obtained by a sol-gel method starting with the rare earth carbonates of Pr, Dy and Er and TEOS (tetraethoxysilane). Expressed in the form  $x\text{Ln}_2\text{O}_3(1-x)\text{SiO}_2$ , the glasses have compositions in the range  $x = 0.009$  to  $0.052$ , which corresponds to 0.9 to 5.2 mol% or up to 23 wt% rare earth oxide as determined by electron microprobe. The glasses were produced by densification at  $800^\circ\text{C}$ . Infrared and visible spectra and magnetic susceptibilities are reported.

### 1. Introduction

The characteristics of binary silica-based rare-earth glasses are of particular interest for optical applications in which silica-based materials with large Verdet constants and lasing ability are required. This is especially important in optical fiber technology, where binary rare-earth silicates are needed to create nonreciprocal devices, such as isolators and circulators, and magnetic field sensors. Of course, glasses with these compositions also are of interest in geological, chemical and other optical fields.

Due to the extremely high melting points of rare-earth oxides and  $\text{SiO}_2$ , however, the preparation of binary rare-earth silicates from melts requires temperatures of  $1800^\circ\text{C}$  or higher. Moreover, the melt method is limited to compositions for which quench techniques are sufficiently fast to avoid phase separation problems. This has caused experimental difficulties and often leads to low-quality glasses [1].

The sol-gel method provides an approach to obtaining binary rare-earth silicates as pure, homogeneous glasses at much lower temperatures than required by conventional melt-quench techniques. There have been several attempts to prepare such glasses using sol-gel methods. Mukherjee et al. [2] prepared glasses by melting compositions which were present originally as crystalline materials or gels, so gels were involved, but since melting was required these cannot be considered sol-gel glasses. Wang and Hench [3] reported the preparation of sol-gel derived silica optical filters, using the DCCA approach, including a rare-earth silicate described as a "1% (mol%) Nd silica gel heated to  $850^\circ\text{C}$ ". However, it carefully was not described as a glass, and its visible spectrum was found to differ significantly from that of the

for the evolution of most of the  $\text{CO}_2$ . This solution was added dropwise over 10–15 min to a stirred solution made by mixing 10.00 g of TEOS and 10 g of absolute ethanol. This corresponds to 0.004 mol  $\text{Pr}^{+3}$  and 0.048 mol Si, and should lead to a glass of composition  $0.04\text{Pr}_2\text{O}_3 \cdot 0.96\text{SiO}_2$ . Its elemental analysis, when dried and densified, showed it to be  $0.052\text{Pr}_2\text{O}_3 \cdot 0.948\text{SiO}_2$ .

All glasses were examined by X-ray diffraction and shown to be amorphous. The elemental compositions of the glasses were determined to within  $\pm 0.01$  wt% by electron microprobe analysis, calibrated with accurately known standard. The microprobe data were measured with a Cameca Microprobe (take off angle  $40^\circ$ ) at an excitation voltage of 20 kV and beam current of 15 nA. Infrared spectra were obtained on a Digilab FTS-15B spectrometer. The KBr pellet technique was used. At least 200 scans at a resolution of  $2\text{ cm}^{-1}$  were signal-averaged. Magnetic susceptibility measurements were performed on a Faraday Balance equipped with a Cahn electrobalance (model RG) at room temperature. Measurements were made at field strength 10.40 kOe and field gradient,  $H(dH/dz)$ , of 17.93. Thermal gravimetric analysis (TGA) was performed on a System 113 thermal gravimetric analyzer. Visible absorption spectra were obtained on a Cary 17 UV/Visible spectrophotometer.

### 3. Results and discussion

The lanthanide silicate glasses prepared by this method were designed to have 0.9 to 5.2 mol% rare earth, where the mol% is given by  $x$  in the formula  $x\text{Ln}_2\text{O}_3(1-x)\text{SiO}_2$ . When they were analyzed after initial densification at  $600^\circ\text{C}$ , with about 2 h at  $800^\circ\text{C}$ , the lanthanide and silicon concentrations were slightly less than expected. The materials contained from 0.2 to 6 wt% of another component, which was assumed to be  $\text{H}_2\text{O}$ , since no chlorine was present. Samples of these materials were studied by thermogravimetric analysis and found to give off volatiles constituting this weight percentage in the  $800\text{--}850^\circ\text{C}$  range when heated over about 3 h. Therefore the glasses were heated further at  $800^\circ\text{C}$  for 10 h and newly analyzed by electron microprobe.

Each glass was analyzed at 10–40 randomly selected  $20\text{ }\mu\text{m}$  regions. The analysis at each spot on a given sample gave identical results. The compositions were determined to an accuracy of  $\pm 0.01$  wt% and are given in table 1. All analyses accounted for  $99.5 \pm 0.5$  wt% of the glasses in terms of  $\text{Ln}_2\text{O}_3$  and  $\text{SiO}_2$ , and are given in table 1 in terms of  $x$  in  $x\text{Ln}_2\text{O}_3(1-x)\text{SiO}_2$ .

The fact that the glasses were X-ray amorphous and the fact that all  $20\text{ }\mu\text{m}$  spots gave identical analyses, show that these materials are amorphous and homogeneous, with no possible phase separation at a level greater than ca  $20\text{ }\mu\text{m}$ .

The infrared and ultraviolet-visible spectra of the glasses were measured. The infrared spectra of one of the glasses,  $x\text{Er}_2\text{O}_3(1-x)\text{SiO}_2$ ,  $x = 0.035$ , taken both after initial and final densification, are shown in the  $500\text{--}1800\text{ cm}^{-1}$  region in fig. 1. The spectrum of the glass taken after treatment at

1220  $\text{cm}^{-1}$ . However, the shapes and relative intensities of these bands differ somewhat from those of  $\text{SiO}_2$ , of course, due to the presence of the rare-earth ions, but no new separate bands are introduced. This is shown in fig. 2, where the 450–1400  $\text{cm}^{-1}$  spectra of a series of dysprosium silicate glasses with increasing Dy content are presented. The main regions of interest are 600–640  $\text{cm}^{-1}$ , where the absorbance decreases slightly as  $\text{Dy}^{+3}$  ions are introduced, and near 900  $\text{cm}^{-1}$ , where the absorbance increases significantly. On close inspection of the spectra in fig. 1 and analogous spectra in which the rare-earth content is constant, it is seen that the decrease occurs near 620  $\text{cm}^{-1}$  as densification occurs, but that no increase occurs near 900  $\text{cm}^{-1}$ . Thus, we believe that the small decrease in the 600–640  $\text{cm}^{-1}$  region is associated with the network, and that the increase at 920  $\text{cm}^{-1}$  is due primarily to the presence of the rare-earth ions. Since the 870–930  $\text{cm}^{-1}$  region is quite typical for the infrared active M–O stretch of oxygens bound to highly charged metal ions [7], the absorbance increase at 920  $\text{cm}^{-1}$ , proportional to the  $\text{Ln}^{+3}$  concentration, is assignable to such a vibration. This assignment must be taken to be tentative, however, in the light of the well-known complexity of silicate spectra.

The glasses treated only to 600°C show evidence of incomplete formation of the network and of the presence of  $\text{H}_2\text{O}$ . Thus, in fig. 1(a) the band at 1620  $\text{cm}^{-1}$  is due to the H–O–H bending mode. It is largely removed by extended heating at 800°C, as shown in fig. 1(b). In regions not shown, the 600°C treated glass also shows the presence of water by a broad absorbance in the 3000–3700  $\text{cm}^{-1}$  region, which is lost upon treatment at 800°C.

The usefulness of a glass as a Faraday rotator depends on both its absorption spectrum and its magnetic susceptibility. The visible absorbance spectrum also serves as a basis for comparison of the ligand fields of the rare-earth ions in these glasses with those in melt-quenched glasses containing them. Although exact comparisons are not available, spectra of rare earths in glasses with other networks can be used. The spectrum of one of the erbium silicate glasses is shown in fig. 3. The bands correspond to the transitions assigned in table 2 and compared to the bands reported for erbium borate glasses [8]. They correspond quite closely, as do those of the praseodymium silicate glass to the transitions found in  $\text{Pr}^{+3}$  in the melt-prepared phosphate glasses [9]. This result can be contrasted to the situation in Nd gels reported by Wang and Hench [3], who found that the spectrum of the gel was quite different from that of the melt-quench glass. Thus, in the sol-gel prepared glasses reported here, the optical absorptions of the rare-earth ions are as expected for fully formed glasses.

The magnetic properties of the rare-earth glasses are central to their potential application. The magnetic susceptibility,  $\chi$ , is strongly related to the Verdet constant, which measures the magnitude of the Faraday effect. The magnetic susceptibilities of these sol-gel prepared glasses are presented in table 1. The values of  $\chi$  reported here are corrected for diamagnetic contributions, and represent the paramagnetic susceptibilities associated with the

magnetically in the network at room temperature. This is the expected behavior for rare-earth ions, whose magnetic properties are due primarily to unpaired electrons in f orbitals. The magnetic moments are quite close to those expected for the  $^3H_4$  state of  $\text{Pr}^{+3}$ , the  $^6H_{15/2}$  state of  $\text{Dy}^{+3}$  and the  $^4I_{15/2}$  state of  $\text{Er}^{+3}$  [10].

The key to success in this sol-gel method involves control of the introduction of the rare-earth ions. Analogous preparations in which there was significantly more  $\text{H}_2\text{O}$  or in which the rare-earth ions were introduced as their soluble chlorides or nitrates were not successful. Moreover, if the initially dissolved rare-earth carbonate was allowed to stand in air for more than 1 h, the efficiency of introduction of the ions (the concentration attainable) decreased significantly. From these results, we infer that the release of  $\text{CO}_2$  by acidification of the carbonate, under the conditions used, leaves the rare-earth ions essentially as hydrated ions which do not form hydroxides, because of the acidity, or other unreactive or insoluble ions, within the time required for addition to the alcoholic TEOS solution. Thus, the key seems to be to obtain ions in concentrated solution (so there is as little water as possible) and to react them with TEOS before they undergo reactions with  $\text{Cl}$ ,  $\text{H}_2\text{O}$  or  $\text{O}_2$  to form unreactive complexes. The stoichiometry is crucial as well, because increasing the amount of  $\text{H}_2\text{O}$  used to dissolve the rare-earth ion serves to limit the concentration of  $\text{Ln}^{+3}$  in the glass by increasing the amount of TEOS solvolyzed. Thus, the stoichiometry and the kinetics of the initial stages of reaction must be controlled. Recognizing the importance of the metal ion coordination chemistry is even crucial to preparing transition metal silicate glasses.

The analysis of these materials not only provided the  $\text{Ln}^{+3}$ , Si and O contents, it also showed that no C or Cl remained in the glasses. This means that HCl is lost completely and that the heating schedule leads to complete evaporation of the ethanol present both as solvent and as a product of solvolysis of the TEOS. The water present in the system was lost more slowly, as indicated by the fact that the last 0.2 to 6 wt% was removed at  $800^\circ\text{C}$ . Presumably it also would be removed, but more slowly, at  $600^\circ\text{C}$ .

In this work the objective was to prepare glasses of controllable composition in the 0–6 mol%  $\text{Ln}_2\text{O}_3$  range by a sol-gel method, and it was found possible to do so without heating above  $800^\circ\text{C}$ . Such lanthanide concentrations represent the range over which a region in an optical fiber would be expected to vary as it progresses radially from a concentrated region to a pure silica region. Moreover, it is near a eutectic at which congruent melting could occur without phase separation, including that due to liquid-liquid micro-phase separation. Since it was not the objective to make monolithic structures, the gel was broken up from time to time during densification (after gel formation) to enhance evaporation of volatile components. This is not necessary in principle, so other macroscopic forms are possible. The materials obtained ranged from small particles to pieces about 0.5 cm in diameter.

# Actinide Silicate Binary Glasses: Low Temperature Sol-Gel Preparation of Uranium and Thorium Silicate Glasses

Wook-Hwan Lee, Kang Sun and William M. Risen, Jr.

Department of Chemistry

Brown University

Providence, Rhode Island 02912

Binary uranium silicate and thorium silicate glasses have been obtained by a sol-gel method starting with the oxides and TEOS (tetraethylorthosilicate). Expressed in the form  $xM_aO_b(1-x)SiO_2$ , the glasses fall in the range; 0.0017 to 0.047, which corresponds to 0.17 to 4.68 mole percent and, for uranium up to 19 weight%  $UO_3$ , as determined by electron microprobe. These elements were incorporated as U(VI) (in the  $UO_2^{+2}$  form) and Th(IV). The glasses were produced by densification at temperatures of 700° C or less. Partial crystallization of uranium silicate occurs on heating at 800° C or above. The infrared and visible spectra are reported.

## Introduction

One approach to storing uranium, plutonium and other actinides from partially spent fuel in fission reactors is to incorporate in glasses the portion that cannot be recycled usefully. The requirements for a successful glass system are demanding, and include high chemical stability of the initially formed glass, long range containment of the actinides and of the materials formed during the decay of the actinides and their fission products, and compatibility with other elements placed into the glass. Optimizing a complete storage

system demands consideration of many other factors as well (1). One such factor is the glass forming process itself, which must be carried out so that the elements are contained during processing. That as well as other materials and energy-related issues tend to make high temperature melt quench or glass sintering processes complex and costly.

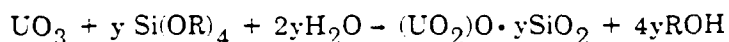
It would be advantageous to have a low temperature, atmospheric pressure way of preparing stable glass containing actinides, lanthanides (2) and other elements present in nuclear waste, and the sol-gel method is one obvious choice. To this end a number of ways of ion exchanging metal ions on silica surfaces (3) coprecipitation and coagulation of colloids, and use of mixed network glass forming solutions (4, 5) have been investigated. It seems clear that both for storage purposes and to obtain materials in which the role of the metals can be studied, it would be advantageous to have a way to prepare stable homogenous binary actinide silicate glasses with a method which does not require the use of reagents that are difficult to handle, containment conditions that are hard to attain, or temperatures that can lead to vaporization of the actinides. In principle it is possible to achieve this by using sol-gel techniques, but no binary silicate glasses of this type have been reported to our knowledge.

In this paper, we report the preparation of homogeneous binary uranium and thorium silicate glasses by sol-gel methods. The chemistry employed to make the uranium silicates containing  $\text{UO}_2^{-2}$  units should be applicable to Np, Pu and Am, as well, since they also form  $\text{MO}_2^{-2}$  species (6). The chemistry of Th and Pa is enough different from that of U that a slightly modified sol-gel method has been employed to obtain binary thorium silicate glasses.

Glasses with the formal composition  $x\text{UO}_3 \cdot (1-x)\text{SiO}_2$  have been prepared in the range  $0 < x \leq 0.047$ , or up to about 5 mole percent  $\text{UO}_3$ . This range corresponds to 0-18.9 weight percent  $\text{UO}_3$  or 0-15.8 weight percent uranium. A 5 mole percent glass of this type would be  $(\text{UO}_2)_5\text{O} \cdot 19 \text{SiO}_2$ . Thorium glasses have been prepared in the range  $0 < x$

$\leq 0.0319$ , or to about 3 mole percent.

The uranium glass synthesis has been designed to incorporate the element in the +6 formal oxidation state, since  $U^{+3}$  is easily oxidized to  $U^{+4}$  by air,  $U^{+4}$  can be oxidized readily and  $U^{+6}$  is quite stable in the form  $UO_2^{+2}$ . The well known stability of  $UO_2^{+2}$  is ascribed to the unusually strong U-O bonds in the linear O-U-O structure. The design also is based on the approach to sol-gel binary silicates we developed for the preparation of lanthanide silicates (2). It involves the reaction of  $UO_3$  (or other sources of the well known uranyl ion,  $UO_2^{+2}$ , and O, such as  $UO_2CO_3 \cdot H_2O$ ) with tetraethylorthosilicate ( $Si(OR)_4$   $R=C_2H_5$ ), and  $H_2O$ . *via* the overall reaction, stated for  $UO_3$  in a form which highlights the presence of  $UO_2^{+2}$ :



While this is a straightforward approach in principle, it is important to recognize that a number of competing processes can occur as the gel is formed or transformed to glass. They could lead to the presence of lower valent oxides in the glass or as separate phases.

The preparation of the thorium glasses proceeds more conveniently in a somewhat different way. Although the oxide,  $ThO_2$ , and certain carbonate species, such as  $Th(OH)_2CO_3 \cdot 2H_2O$ , can be sources of the oxide, thorium hydroxide is more appropriate. Two forms of " $Th(OH)_4$ " can be precipitated from  $Th(NO_3)_4$  solutions by alkali hydroxide (7). One of them is a hydrated amorphous gel containing  $Th(OH)_4$  tetrahedra that are weakly connected by H-bond bridges. It is stable thermally, and, although it can pick up ambient  $CO_2$  to form the hydrated hydroxycarbonate, it is readily soluble in HCl.

### Experimental

The glasses were made by combining two solutions, A and B, to form a solution, that was allowed to gel and then dried and densified. Solution A was prepared by dissolving

TEOS, tetraethylorthosilicate (or tetraethoxysilane)  $(\text{Si}(\text{OC}_2\text{H}_5)_4)$  (Aldrich) in absolute ethanol,  $\text{C}_2\text{H}_5\text{OH}$ . Solution B was prepared by dissolving  $\text{UO}_3$  (or  $\text{Th}(\text{OH})_4 \cdot z\text{H}_2\text{O}$ ) in a minimum of 12M HCl, adding  $\text{H}_2\text{O}$  and dissolving this solution in absolute ethanol. Solution B was added dropwise with stirring to solution A over a period of about 5 minutes beginning within 5 minutes of preparation of solution B. The homogeneous solution which was formed gelled in a loosely covered beaker in 8-10 hours at  $25^\circ\text{C}$ . The gel was cured at  $25^\circ\text{C}$  for 6-14 days. Then it was heated slowly (ca  $1^\circ\text{C}/\text{min.}$ ) from  $25^\circ\text{C}$  to  $600^\circ\text{C}$  ( $700^\circ\text{C}$  for Th) and held at  $600^\circ\text{C}$  for periods ranging from 2 hours to 64 hours ( $700^\circ\text{C}$ , 24 hr. for Th).

In a typical preparation of the "5" mole percent glass, 0.7226g ( $2.525 \times 10^{-3}$  mole) of  $\text{UO}_3$  was added to 1.0g 12M HCl and 5.184g  $\text{H}_2\text{O}$  with stirring and allowed to react for one minute. This solution was added to 5.0g absolute ethanol to form solution B. Solution B was added dropwise with vigorous stirring to a polypropylene beaker containing solution A, 10.00 g TEOS and 5.0 g absolute ethanol, over a 5 minute period. When addition was complete the beaker was loosely capped and stirring was continued until gelation had occurred (about 8 hours). The gel was allowed to age on standing for 8 days. The gel was transferred to a platinum crucible and placed in a temperature programmed furnace whose temperature was raised at  $1^\circ\text{C}/\text{min.}$  to  $600^\circ\text{C}$ . It was held at  $600^\circ\text{C}$  for 64 hours and the glass was removed for analysis. Electron microprobe analysis showed it to contain 4.68 mole percent  $\text{UO}_3$ . The difference between 4.68 and the theoretical content of 4.97 mole percent results from the presence of some  $\text{UO}_3 \cdot 2\text{H}_2\text{O}$  in the  $\text{UO}_3$  reactant.

To make thorium silicate glasses, thorium hydroxide, " $\text{Th}(\text{OH})_4$ ", was made from thorium nitrate,  $\text{Th}(\text{NO}_3)_4 \cdot 4\text{H}_2\text{O}$ . Excess aqueous sodium hydroxide (0.06 mol, 2.4g) was added to an aqueous solution of 5.5212g (0.01 mol) of thorium nitrate,  $\text{Th}(\text{NO}_3)_4 \cdot 4\text{H}_2\text{O}$ , with stirring, to produce the white  $\text{Th}(\text{OH})_4 \cdot z\text{H}_2\text{O}$  gel. The gel was separated, washed with water 5 times, and dried at  $120^\circ\text{C}$  for 1 day. As discussed

above, this resulting material is hydrated  $\text{Th}(\text{OH})_4$ , but it can become carboxylated partially on standing.

In a typical preparation of the "3" mole percent thorium silicate glass, 0.4453 g (which corresponds to  $1.484 \times 10^{-3}$  mole on the basis of " $\text{Th}(\text{OH})_4$ ") was dissolved in 1.2 g 12 M HCl, and 5.184 g  $\text{H}_2\text{O}$  and 5.0 g of absolute ethanol were added to form solution B. Solution B was added dropwise over 5 min to stirred solution A, made by mixing 10.00 g of TEOS and 5.00 g of absolute ethanol. The resulting solution (sol) gelled in about 10 hours in a loosely closed beaker in air. The gel was aged at  $25^\circ\text{C}$  for 5 days, and then heated to  $700^\circ\text{C}$  at a controlled heating rate of  $1^\circ\text{C}/\text{min}$ . It then was densified at  $700^\circ\text{C}$  for 24 hours to convert it fully to glass. Electron microprobe analysis showed it to contain 2.63 mole percent  $\text{ThO}_2$ , as would be the case if the thorium hydroxide corresponded to the trihydrate,  $\text{Th}(\text{OH})_4 \cdot 3\text{H}_2\text{O}$ .

The glasses were analyzed by x-ray diffraction, infrared and visible spectroscopy, and electron microprobe techniques. The infrared spectra were measured on powdered samples dispersed in KBr pellets using an IBM IR-98 Fourier Transform infrared spectrometer. The visible spectra and near infrared (300-1400 nm) were measured on ground and polished thin glass sections of cross section  $\text{ca } 5 \text{ mm}^2$  using a Cary 17 UV-visible spectrometer. The electron microprobe measurements were made on 5-20 randomly selected 15 micron spots using a Cameca Microprobe (take off angle  $40^\circ$ ) at an excitation voltage of 15 KV and beam current of 10.3-10.6 nA. The metal and silicon contents were probed and the compositions were calculated on the bases of  $\text{UO}_3$  or  $\text{ThO}_2$  and  $\text{SiO}_2$ , since oxygen was not measured. Total compositions accounted for nearly 100 weight percent, eg (98.6-99.4) in the case of uranium glasses, using melt-synthesized multicomponent glasses for references.

## Results and Discussion

The preparation of the starting solutions proceeded smoothly, and the gels formed with steadily increasing viscosity until brittle solids were obtained. After aging, the uranium-containing gels were heated at  $1^{\circ}\text{C}/\text{min}$  to  $600^{\circ}\text{C}$ , to remove  $\text{H}_2\text{O}$ ,  $\text{C}_2\text{H}_5\text{OH}$  and  $\text{HCl}$ , and then heated at  $600^{\circ}\text{C}$  for 2-64 hours. In the case of thorium, the gels were heated similarly to  $700^{\circ}\text{C}$  and then heated at that temperature for 24 hours.

The x-ray scattering of powdered samples showed them to be x-ray amorphous. The compositions of the glasses, obtained in terms of their Th or U to Si ratio by microprobe are given in Table 1, and expressed for the dehydrated samples on the basis of  $\text{MO}_3$  (or  $\text{MO}_2$ ) and  $\text{SiO}_2$ . The infrared spectra confirmed that they are nearly free of  $\text{H}_2\text{O}$  and  $\text{HCl}$  within the detection limits inherent to the technique used to disperse a crushed powder in KBr for measurement of the spectra of the pellets. This is shown for the case of the USi300 glass in Figure 1, where the entire infrared spectrum is displayed from  $3500$ – $500\text{ cm}^{-1}$ . The expanded scale infrared spectra of the 0.73, 2.90 and 4.68 mole percent  $\text{UO}_3 \cdot \text{SiO}_2$  glasses are shown in the  $600$ – $1800\text{ cm}^{-1}$  region in Figure 2, and the visible spectra of the latter two are shown in Figure 3 in the  $300$ – $600\text{ nm}$  region. No absorption bands were observed in the  $600$ – $1400\text{ nm}$  region.

The ultraviolet visible spectrum of 2.90 and 4.68 mole percent  $\text{UO}_3 \cdot \text{SiO}_2$  glasses in the  $320$  –  $700\text{ nm}$  region exhibit a band centered at  $425\text{ nm}$  and the onset of stronger absorption at shorter wavelength. Uranium ions have distinctive visible spectral features, which have been analyzed in detail for the various oxidation states with a wide range of ligands in crystalline, solution, gas phase and amorphous states. The common characteristic of systems containing uranyl,  $\text{UO}_2^{+2}$ , ions is a reasonably intense ( $\log \epsilon \sim 1$ – $2$ ) band centered in the  $410$ – $450\text{ nm}$  region. This is widely observed in glasses containing  $\text{UO}_2^{+2}$  (8). The band appears at  $418\text{ nm}$  (peak maximum) ( $415\text{ nm}$ ) and center in aqueous  $\text{HClO}_4$  solutions (9), while in crystals or non-aqueous solutions in which the  $\text{UO}_2^{+2}$  ion has associated anions, eg.  $\text{UO}_2(\text{NO}_3)_3^-$ , the band is shifted to longer

wavelengths with the band center nearer to 450 nm (10). When the nearest neighbor environment is ordered, the vibrational structure of the electronic transition is resolved, but when the  $\text{UO}_2^{+2}$  ions are distributed over a range of types of neighboring sites the environment is reflected in asymmetry of the band. The presence of a somewhat asymmetric band at 426 nm thus is consistent with absorbance due to  $\text{UO}_2^{+2}$  ions in a range of environments which are comprised of oxygens which, on average, exert a ligand field that is somewhat more negatively charged than that of six equatorial  $\text{H}_2\text{O}$  molecules but somewhat more positive than that of three  $\text{NO}_3^-$  or  $\text{CH}_3\text{CO}_2^-$  ions at the optimum spacings they assume in crystals (11, 12) or dissolved complex ions.

The visible spectral features, including the high frequency absorbance due to the onset of the bands known as B and C of  $\text{UO}_2^{+2}$  (9, 13) thus are consistent with the presence of uranyl ions in disordered silicate environments having a net charge of -2 and containing two nonbridging (NBO) oxygens (one on each of two Si atoms) and four bridging Si-O-Si oxygens at average U-O distances greater than the 2.5 Å at which the oxygens of  $\text{UO}_2 \cdot \text{CH}_3\text{CO}_2 \cdot 3$ , for example, appear in the equatorial plane of discrete complex ions (12). There are, no doubt, in the distribution of sites some with oxygens present on Si attached to two NBO's as well, but there is not yet evidence of their presence in large proportion. There is no evidence in the spectra for either U(VI) uranate species, which would be expected near 540 nm, or for U(V) or U(IV) which would have absorbances in the 700-1400 nm region.

The infrared spectra of the uranium silicate glasses shown in Fig 2, support this interpretation. As the concentration of  $\text{UO}_2^{+2}$  is increased several features of the spectrum change. The high frequency shoulder of the main  $\text{SiO}_2$  band centered at  $1100 \text{ cm}^{-1}$  becomes more pronounced, as expected from the introduction of Si-O stretches at silicon sites with one non-bonding oxygen. In addition, a small band grows in at ca.  $900 \text{ cm}^{-1}$  and the main band broadens somewhat to the low frequency side. The latter small

effect is assigned to the presence of a very low concentration of Si with two NBO's and possibly to vibrations of glass network oxygens in the neighborhood of the  $\text{UO}_2^{-2}$  ion. The principal new band is that at *ca*  $900\text{ cm}^{-1}$ , precise position  $888\text{ cm}^{-1}$ , which is assigned to the asymmetric stretch  $\nu_2$  of a nearly linear  $\text{UO}_2^{-2}$  ion. This mode appears at  $895 - 910\text{ cm}^{-1}$  in the spectra of the  $\text{UO}_2^{-2}$  salts and solutions. It is infrared active and would be ungerade in the fully linear species. Thus, it is not the primary contributor to the vibrational structure of the electronic transition near  $420\text{ nm}$ , which is between ungerade states and thus requires the gerade vibration ( $\nu_1$ ), which is at *ca*  $555\text{ cm}^{-1}$  in the ground and  $715\text{ cm}^{-1}$  (ave) in the excited electronic states (9). The infrared active  $\nu(\text{U-O})$  of  $\text{UO}_2^{-2}$  is well known and has been analyzed for a wide range of uranyl salts, and has been correlated to the  $\text{R(U-O)}$  distance by Veall, *et al* (14) and Siegel (15) by the expression  $\text{R(U-O)} = 81.2 \nu^{-2/3} + 0.85$ . From the  $888\text{ cm}^{-1}$  band, the  $\text{U-O}$  distance is found to be  $1.72\text{ \AA}$  for these glasses. This compares well to the value  $1.71\text{ \AA}$  found in  $\text{NaUO}_2\cdot\text{O}_2\text{CCH}_3\cdot 3$

The visible spectrum of the clear, colorless thorium silicate glasses is featureless, of course, but the infrared spectra exhibit absorption in the  $600\text{--}1400\text{ cm}^{-1}$  region. These spectra are similar to those of the uranium glasses except that there is no band at  $900\text{ cm}^{-1}$  or analogous to it since  $\text{Th-IV}^{+}$  does not form an analogous ionic  $\text{MO}_2$  species.

Upon heating the uranium glasses at  $500^\circ\text{C}$  for 2 - 24 hours they darken to a deep orange color, and with extended heating at  $500^\circ\text{C}$  or at higher temperature they eventually acquire a very deep coloration which makes them appear black. Some evidence of crystallization first appears with extended heating at  $700^\circ\text{C}$ . All appear homogeneous under  $40\times$  microscopic examination. However, x-ray study of powders of these materials shows that they contain crystalline components. While it is not obvious that crystallization should occur in this temperature range, the uranium oxide phase diagram (15) shows that for  $\text{UO}_x$  compositions near  $x = 2$ ,  $\text{UO}_2$  is transformed to a mixture of  $\text{UO}_3$  and  $\text{U}_3\text{O}_8$  and

that a range of crystalline uranium oxide compositions can be formed. The crystalline components formed at 800°C appear to be  $\text{UO}_{2.9}$  by x-ray powder pattern, but presumably  $\text{UO}_{2.917}$  or  $\text{U}_{12}\text{O}_{25}$  and  $\text{U}_3\text{O}_8$ . These transformations and concomitant silicate composition and changes occur as the time of heating at 800°C is increased.

The key features of this method are control of the amount of  $\text{H}_2\text{O}$  available for gelation and kinetic control of the form of the metal-containing ion. If there is too much water available, the concentration of Si-OH moieties is increased in the initial stages of the reaction and tends to favor  $\text{SiO}_2$  formation and exclusion of the cation. The latter control is exerted in order to combine a form of the ions in which the ligands to be replaced are  $\text{H}_2\text{O}$  or its fragments or are labile on the gelation time scale. It can be exerted by acid hydrolysis of either a carbonate, leading to exclusion of  $\text{CO}_2$ , or an oxide which is soluble in an acid whose anion is weakly ligating and which acid vaporizes but does not decompose upon drying and densification of the glass. In the present preparation HCl was used as the acid.

Since the more common way to introduce metal ions by a sol-gel method is to react metal alkoxides with TEOS, or another network former, it is useful to consider the feasibility of introducing U(VI) or Th(IV) in that manner. Gilman et al. 17 have reported the preparation of U(VI) alkoxides, which could be used in this way. Uranium VI ethoxide, prepared by oxidizing U(VI) ethoxide by benzoyl peroxide, is a red liquid which can be distilled under vacuum at 75°C and is soluble in a range of organic solvents. It is extremely moisture sensitive and hydrolyzes to give solutions containing the  $\text{UO}_2^{+2}$  ion. Thorium also forms substituted alcoholates, which may be useful precursors. While these approaches may yield interesting materials, the chemistry is much more involved than that used in this work.

Studies to determine the properties of these binary actinide silicate glasses related to their potential role in nuclear waste storage, in particular the synthesis of multicomponent

silicates based on complex mixtures of actinides, rare earths and other important metals. will be reported separately.

### Acknowledgements

We are grateful to Mr. Sen Yang, Mr. Joon Kim, Dr. Ahn and Dr. Long, for their assistance to Professor Aaron Wold and Professor Theodore Morse for their cooperation, and to Dr. Joseph Devine for his electron microprobe measurements. We gratefully acknowledge the support of this work by the AFOSR under contract AFOSR-85-0304 and by the Materials Research Laboratory of Brown University.

Table 1  
Composition of Typical  $x\text{AcO}_n(1-x)\text{SiO}_2$  Glasses

Glass No.	n	mole % $\text{AcO}_n$	Weight % $\text{AcO}_n$	Mole % $\text{SiO}_2$	Stoichiometry
ThSi 025	2	0.17	0.75	99.8	$0.0017\text{ThO}_2 \cdot 0.998\text{SiO}_2$
ThSi 200	2	1.64	6.73	98.36	$0.0164\text{ThO}_2 \cdot 0.984\text{SiO}_2$
ThSi 300	2	2.63	10.62	97.37	$0.0263\text{ThO}_2 \cdot 0.974\text{SiO}_2$
ThSi 500	2	3.20	12.66	96.8	$0.032\text{ThO}_2 \cdot 0.968\text{SiO}_2$
USi 100	3	0.73	3.36	99.3	$0.0073\text{UO}_3 \cdot 0.993\text{SiO}_2$
USi 300	3	2.90	12.43	97.1	$0.0290\text{UO}_3 \cdot 0.971\text{SiO}_2$
USi 500	3	4.68	18.94	95.3	$0.0468\text{UO}_3 \cdot 0.953\text{SiO}_2$

## References

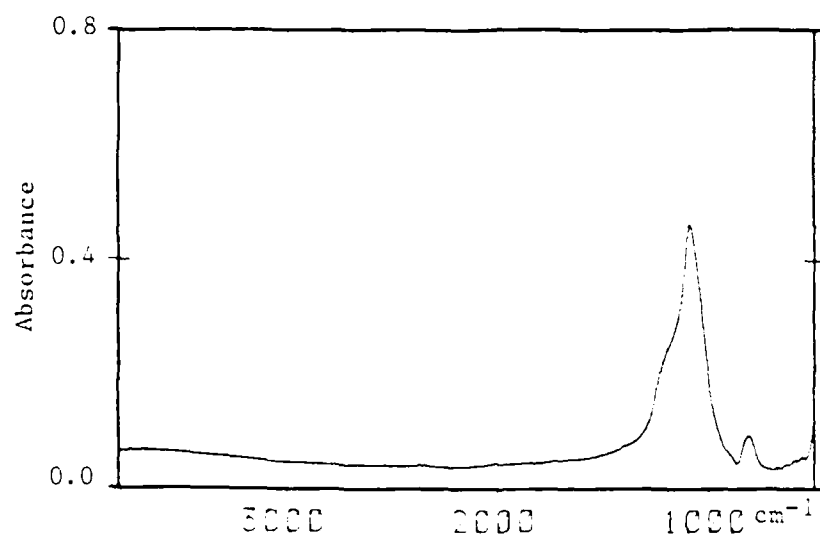
1. Scientific Basis for Nuclear Waste Management V, Ed. W. Lutze, Materials Research Society Symposia Proceedings, v. 11, Elsevier Science Publishing Co., New York, 1982
2. K. Sun, W. H. Lee and W. M. Risen, Jr., *J. Non-Cryst. Solids* 92 (1987) 145.
3. P. B. Macedo, C. J. Simmons, D. C. Tran, N. Lagakos and J. Simmons, U. S. Patent 4,312,744 (1982).
4. E. M. Rabinovich, D. W. Johnson, Jr., J. B. MacChesney, and E. M. Vogel, *J. Am. Ceramic. Soc.*, 10, (1983) 683.
5. J. P. Pope, MRS Meeting, Paper N4-2, Boston, 1982, as described by J. D. Mackenzie, Chapter 2, in *Ultrastructure Processing of Ceramics, Glasses and Composites*, Ed. L. L. Hench and D. R. Ulrich, Wiley-Interscience, New York, 1984.
6. J. Katz, G. T. Seaborg and L. R. Morss, *The Chemistry of the Actinide Elements*, 2nd Ed., Vol 1, Chaps 3, 5 (1986).
7. L. I. Katzin in *The Chemistry of the Actinide Elements*, 2<sup>nd</sup> Edn, Vol I, ed. J. K. Katz, G. T Seaberg and L. R. Morss, Chapman and Hall Publ., New York, 1986, Sect. 3.7.5.
8. H. . Schreiber and G. B. Balazs, *Phys. and Chem. Glasses*, 23 (1982) 139.
9. J. T. Bell and R. E. Biggers, *J. Mol. Spectrosc.* 25(1968)312.
10. L. Kaplan, R. A. Hildebrandt and M. Ader, *J. Inorg. Nucl. Chem.* 2 (1956) 153.
11. I. Fankuchen, *Z Krist.*, 91 (1935) 473.
12. I. I. Chernzayer (1966) *Complex Compounds of Uranium* (Transl. from the Russian by L. Mandel, Israel Program for Scientific Translation Jerusalem).
13. G. H. Dieke and A. B. F. Duncan, *Spectroscopic Properties of Uranium Compounds*, Natl. Nucl energy Ser. Div. III, 2, McGraw-Hill, NY 1949.
14. B. W. Veall, et. al. *Phys. Rev. B* (1975) 12, 5651.
15. S. Siegel, *J. Inorg. Nucl. Chem.* 1978 40, 275.
16. H. R. Hoekstra, S. Siegel and E. X. Gallagher, *J. Inorg. Nucl. Chem.* 32 (1970) 3237.
17. R. G. Jones, E. Bindschadler, D. Blune, G. Karmas, G. A. Martin, Jr., J. R. Thirtle, and H. Gilman, *J. Amer. Chem. Soc.* 78 (1956) 6027.

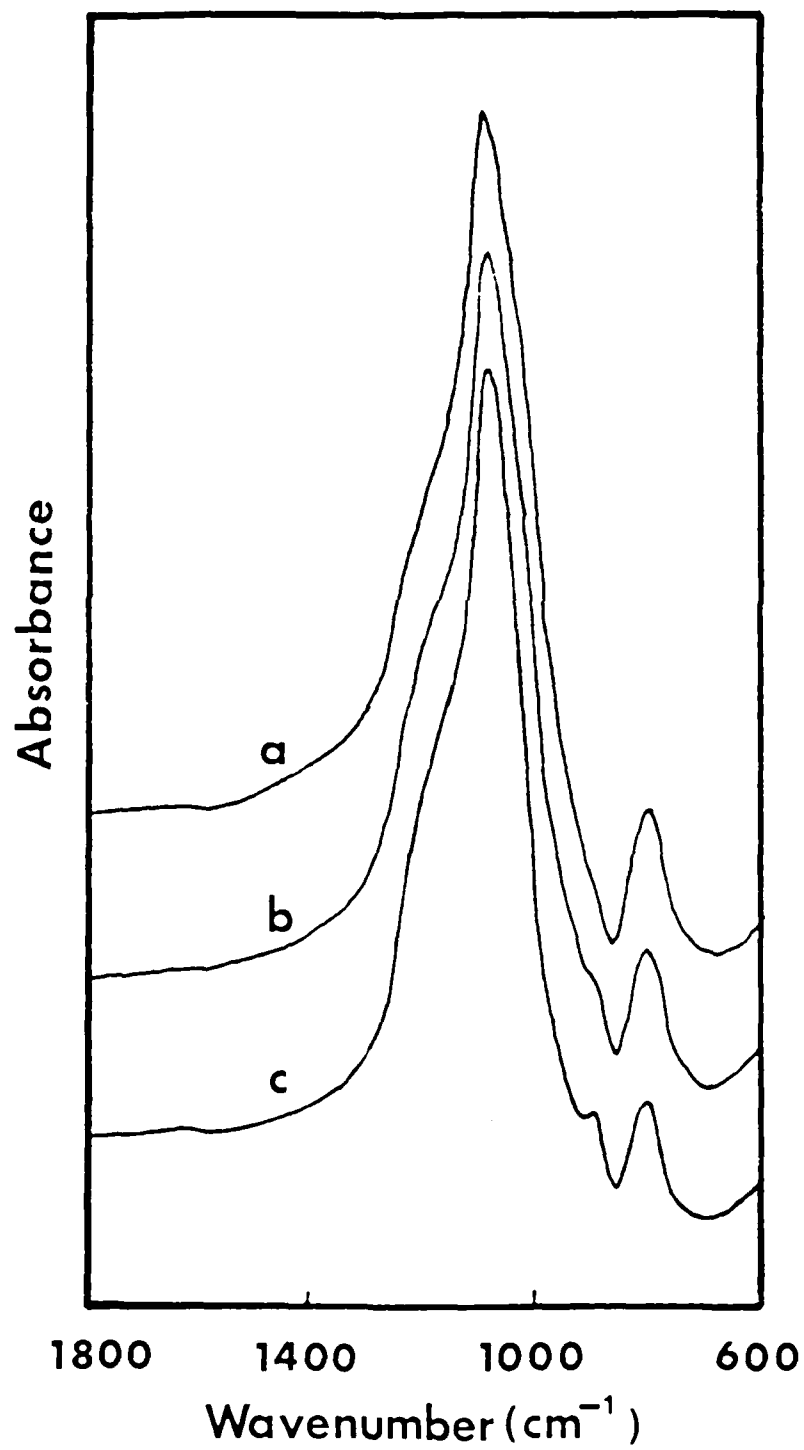
**Figure Captions**

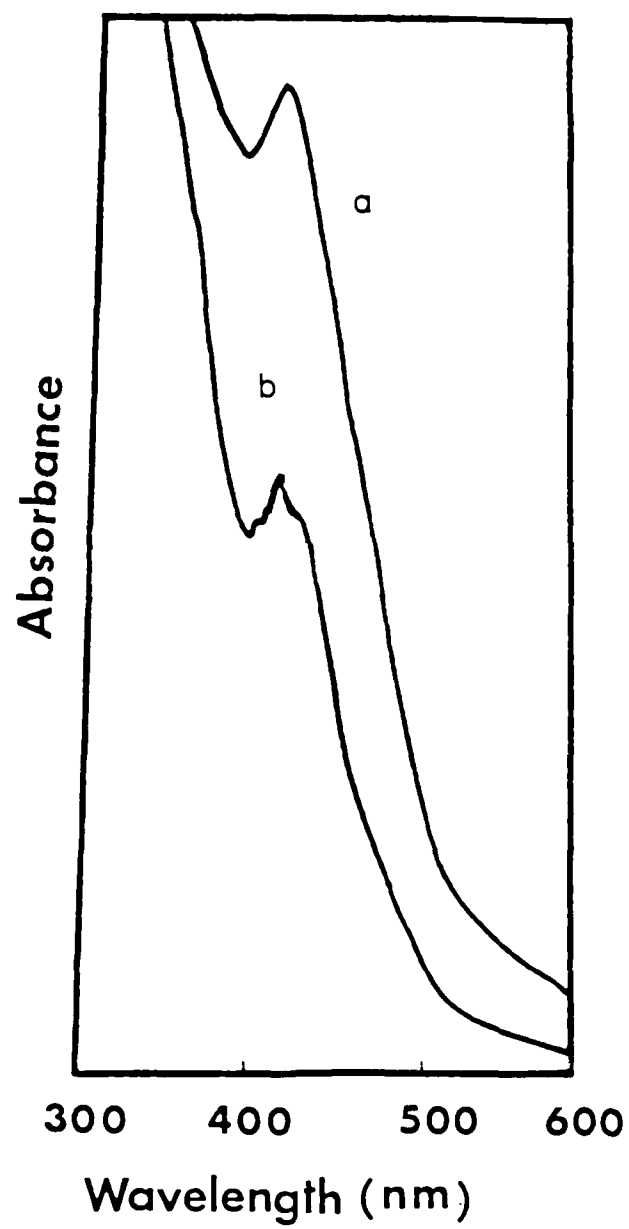
Figure 1. Infrared spectrum of the uranium silicate glass,  $x\text{UO}_3 \cdot (1-x)\text{SiO}_2$ , with  $x = 0.029$  in the  $500\text{--}3500\text{ cm}^{-1}$  region. The baseline due to the KBr in the pellet has not been subtracted.

Figure 2. Infrared spectra of uranium silicate glasses,  $x\text{UO}_3 \cdot (1-x)\text{SiO}_2$ , with  $x = 0.007$  (a), 0.029 (b), and 0.047 (c), in the  $600\text{--}1800\text{ cm}^{-1}$  region.

Figure 3. Visible absorbance spectra of thin sections of uranium silicate glasses,  $x\text{UO}_3 \cdot (1-x)\text{SiO}_2$ , with  $x = 0.047$  (a) and 0.029 (b), in the  $300\text{--}600\text{ nm}$  region. The thickness differ.







## **Appendix: Laboratory for Lightwave Technology**

**Division of Engineering, Brown University, Providence, R.I. 02912**

### **Introduction**

A Laboratory for Lightwave Technology has been established within the Division of Engineering at Brown University. This facility consists of an MCVD (Modified Chemical Vapor Deposition) laboratory, a fiber characterization laboratory, and an optical fiber draw tower. Brown is one of the few U.S. universities at which it is possible to design and fabricate novel optical fibers for sensor and other opto-electronic applications. This equipment presently represents a total of nearly a million dollars in our laboratory alone, and it is supplemented by NMR and Raman equipment for bulk characterization of inorganic glasses in the Departments of Physics and Chemistry. Research is being carried out in cooperation with faculty from the Department of Chemistry, Physics, and also with faculty and staff from electrical and materials engineering. In addition, cooperative research is in progress with the University of Illinois, Northeastern University and two laboratories in the Ruhr University, Bochum, Germany.

Our research program emphasizes new techniques of preform fabrication, the study of specially doped preforms for use as sensors, fiber lasers, polarization maintaining fibers, studies of stress induced effects in fibers, and nonlinear phenomena in fibers. We are also engaged in NMR and Raman studies of the incorporation of novel as well as traditional dopants and how processing affects the manner in which these dopants are incorporated into a glass matrix. Emphasis is placed not on the traditional telecommunications fiber, but on special fibers and fibers associated with sensor applications.

The use of specialty optical fibers as sensors in such disparate fields as solid mechanics, chemical species detection, biology and medicine, creates a seemingly endless list of possible areas of application. We are clearly not in a position to pursue active research into all of the areas in which we believe optical fibers will play an increasingly important role. Our main thrust will be to develop a fundamental understanding of the material and structural attributes of specialty fibers. We also hope to initiate a program in non-linear effects in fibers and to study the effects of novel dopants on Raman gain. As can be seen, the unique

advantages offered by the Laboratory for Lightwave Technology can only be utilized with participants who can contribute to the multidisciplinary aspects of the research.

A series of proposals have been written and submitted to various agencies with the intention of supporting joint activity outside of our group in the Division of Engineering. At the present time, there are four Ph.D. students within the Division of Engineering and one in the Department of Chemistry associated directly with the activities of our laboratory. It is expected that this number will double in the near future. Participants in the activities of our laboratory include Prof. K.S. Kim (University of Illinois), an expert in both optics and solid mechanics, and Prof. J. Cipolla, a professor of Mechanical Engineering from Northeastern University who has been closely involved with the theoretical aspects of this work. The faculty at Brown University are: two professors of chemistry; Prof. W. Risen, an expert in amorphous glasses, and Prof. A. Wold, a chaired professor and editor of the *Journal of Solid State Chemistry*; Prof. N. Lawandy, from electrical engineering (recipient of a Presidential Young Investigator award from the National Science Foundation), and Prof. B. Caswell, and Prof. E. Suuberg, two professors from the Fluid Mechanics, Thermodynamics and Chemical Processing group; Prof. P. Bray, a chaired professor from the physics department specializing in NMR studies of glasses. All will be contributing their expertise toward increasing our understanding of various materials and fabrication problems as well as applications of lightguides. In addition, Prof. Stiles (strained super lattice semiconductors), Prof. Nurmikko, (ultra-fast optical processes in semiconductors), and Prof. Rosenberg (fast electronic devices) are participating in a cooperative program involving semiconductor/fiber devices. We are also collaborating on some novel concepts of "soot" deposition with Prof. M. Fiebig of the Ruhr Universitaet, Bochum, Germany.

### **Research Topics**

Although there are several techniques for the fabrication of high performance, low loss optical fibers such as OVPO (external deposition, Corning Glass), PCVD (microwave discharge, internal, Phillips), MCVD (internal, AT&T and Bell Laboratories), and VAD (vapor axial deposition, Japan), they all have in common the deposition of glass from reactions that occur in the vapor phase. Perhaps the most flexible of these techniques is

MCVD (Modified Chemical Vapor Deposition). This is the process that will be used in our laboratory in the fabrication of novel lightguides for sensor applications.

In the following, we list several research topics and support for our present program. Since our facility enables us to design and fabricate fibers for a variety of purposes, other topics not cited here may well be pursued in the future.

#### [ 1.] Rare Earth Doping of Optical Fibers

There is great interest in the doping of fiber preforms with rare earth elements. (AFOSR Physics Branch, \$280,000, 24 months) These rare earth elements are difficult to obtain in the vapor phase, and we hope to introduce a novel procedure for the incorporation of rare-earth dopants into a silica matrix. First, however, it is perhaps appropriate to discuss, albeit briefly, the motivation behind this project.

When light propagates through a glass doped with these elements its electric field vector rotates by an amount proportional to the strength of an external magnetic field and the length of interaction. The constant of proportionality is called the Verdet constant, which is large for the rare earth elements. By sensing the rotation of the field, fibers doped with such materials can be used as electric and magnetic field sensors. In addition, the rotation of the electric field within the fiber (in the presence of a magnetic field) allows the creation of non-reciprocal devices such as isolators and circulators, which are now in common use in the microwave region. One of the possible barriers to the fabrication of such devices is the difficulty of incorporating the lanthanide elements into a silica based glass in the vapor phase. The group at Southampton (D. Payne, S. Poole, et.al.) have developed a double burner technique for introducing rare earth chlorides into the MCVD gas stream, and have produced a host of fiber lasers. (J. Lightwave Technology, July 1986) The disadvantage of this technique is that it is difficult to obtain axial uniformity in the dopant. An alternate procedure used by this group, as well as by the group at AT&T Bell Laboratory, is to de-mount the preform from the glass lathe, immerse it for several hours in an aqueous solution containing the desired rare earth salt, and then dehydrate the tube. Since the rare earth salts of interest (in particular Nd) are soluble in polar organic liquids, we plan to consider the introduction of the rare earth salts in polar fluor-carbons in the form of an aerosol spray. This would eliminate the problem of axial non-uniformity

as well as the lengthy dehydration time. The focus of this research will be in a study of fiber sensing devices and fiber lasers.

## [ 2.] Second Harmonic Generation in Silica Based Fibers

This work is being carried out in conjunction with Major J. Rotger, Frank J. Seiler Laboratory, U.S.A.F., Colorado Springs, and Dr. Ulf Osterberg, of Prof. Stegeman's group at the University of Arizona.

Second harmonic frequency generation can occur in transparent materials lacking a particular center of symmetry. In these materials, it is possible for two photons of frequency  $\omega$  to interact with a lattice to produce one photon of frequency  $2\omega$ . In certain non-linear crystals, the efficiency with which this can be done depends on a host of parameters such as crystal orientation, phase matching conditions, and can be as high as 40%. These crystals can be quite expensive, of the order of several hundred to several thousand dollars. Such crystals are in common use in a host of lasers, and, in particular, in the Nd:YAG laser. This doubles the frequency from  $1.06 \mu$  to  $.53 \mu$  where, in the green, the radiation can serve as a pump for dye lasers. Such frequency doubling with an intra-cavity nonlinear crystal can perhaps also be used in conjunction with a tunable alexandrite laser.

There are a host of applications for nonlinear optical elements capable of frequency doubling, or frequency mixing, and, unfortunately, these effects, until quite recently have been seen only in crystalline materials. A particular geometry in which such devices could be particularly exploited is that of an optical fiber. Since the fibers are so small, the outer diameter of the order of  $100 \mu$ , it is possible to achieve high intensities needed for the generation of such nonlinear effects even with diode lasers. However, it can be shown that second harmonic generation can not be produced in isotropic materials since  $\chi_2$  is essentially zero. For this reason, there have been attempts to grow crystal fibers and to exploit the strain induced asymmetry of polarization maintaining fibers in the hope of obtaining fibers capable of nonlinear effects. The advantage of fibers, in particular fibers of amorphous as opposed to crystalline material, is that they can be inexpensively produced in large lengths.

Thus, what would be most desirable is a fiber fabricated with the techniques developed by the optical fiber industry (MCVD), that will exhibit the needed asymmetry of structure

to obtain second harmonic generation. A series of experiments (Osterberg and Margulis, Optics Letters, August 1986, February 1987) have recently indicated such a possibility by creating anisotropic radiation induced defects in a silica based fiber with phosphorous doping in the core as well as the cladding. The raised core index was from germanium doping. These experiments indicate an exciting possibility of studying not only fundamental aspects of radiation induced anisotropies in glass, but of taking advantage of this phenomenon for a host of nonlinear fiber devices.

The experiment was fundamentally simple. (Osterberg and Margulis, 1986, 1987) A cw modelocked Nd:YAG laser was Q switched to provide 100-130 psec pulses in Q switched trains that lasted for 250 nsec (FWHM). This  $1.06 \mu$  radiation was focussed into a fiber, described above. Since the  $\chi_2$  coefficient is zero for a glass, no second harmonic generation was noted. However, after a period of several hours of pumping with this source, the light in the output was green, indicating a frequency doubling. This output in the green increased exponentially with time until saturation was reached after about twelve hours of pumping with the Nd:YAG laser. The conversion efficiency was 5%, and occurred only with phosphorous doping in the core as well as in the cladding. The pumping laser was polarized, and the nonlinear doubling seemed to emanate from the portion of the fiber from 20-40 cm. Beyond this length, no further frequency doubling occurred, and the pump and frequency doubled component did not interact with one another. Speculation might lead one to conclude that in the first 20 cm of fiber cladding modes interfered with the phase matching condition that was naturally present. Following this section, the green light was no longer coherently coupled to the pump source, and frequency doubling did not occur.

A possible mechanism for this nonlinear action might well be found in the fact that the polarized pump beam could induce defects that would destroy the symmetry of the material, and thus create a  $\chi_2$ . A recent article by Stolen and Tom (Optics Letters, August 1987) proposes a theory for the existence of this new phenomena of second harmonic frequency generation. The experiments performed by this group found, however, only 1% efficiency of frequency doubling, as contrasted with the 5% obtained by the Swedish group. It is clear that there is much to be done, both theoretically and experimentally in this area, and our laboratory is uniquely suited to pursue this topic.

Supported by the National Science Foundation: \$222,000, three years. We have shown that laser heating of the aerosol deposited in the MCVD (Modified Chemical Vapor Deposition) fabrication of the preforms from which optical fibers are formed can have a dramatic effect on both the rate and quality of deposition. With equipment that will allow us to create state-of-the-art optical fiber preforms, we plan to study the effects of laser enhanced thermophoretic deposition on optical fiber preforms and the fibers pulled from these preforms. In addition, we will study the collapse rate of preform tubes with the addition of axial laser radiation from a 250 W Model 410 Coherent Radiation carbon dioxide laser. We plan to examine this phenomenon experimentally and theoretically. Increasing the diameter of preform tubes to obtain more fiber can increase the time of tube collapse considerably, and a study of the influence of internal laser heating may yield information on how this step in optical fiber fabrication can be shortened. Much effort has been spent in the development of computer codes, including three dimensional effects, that describe fundamental heat and mass transfer processes in MCVD. The results of this work have appeared in publications that such as the Journal of Heat Transfer, Journal of Colloidal and Interfacial Sciences, Journal of the Ceramic Society, to the Journal of Lightwave Technology.

#### 4.1 NMR Studies of Vapor Deposited Preforms and Fibers

Several techniques will be used to gain an assessment of the structure of the fibers fabricated in our laboratory. One of these, NMR (Nuclear Magnetic Resonance), will be employed in a fundamental study of the incorporation of dopants into optical fibers. Prof. P. Bray, of the Department of Physics will be guiding this aspect of the program. It is of great interest to characterize and possibly explain the differences between glasses formed from the melt, and those formed from vapor phase deposited glasses. This is particularly true for an understanding of the radiation induced damage associated with nonlinear second harmonic generation in silica based fibers. Having already made some silica based fibers with phosphorous doping in the cladding as well as the core, we plan to examine the effect of Nd:YAG radiation on the microstructure of the phosphorus bonding to determine the exact symmetry breaking conditions that permit second harmonic generation in an ostensibly isotropic, amorphous material.

Measurements of dipolar broadening, quadropolar effects, chemical shifts, and spin-lattice and spin-spin relaxation times will be used to determine whether dopants (or glass components) are aggregated or dispersed, and to characterize the bonding configurations and structural groupings formed in the glasses.

Studies are already in progress involving boron and fluorine in fibers provided from industrial sources. Detailed studies of phosphorous in silica fibers have been published from another laboratory. Since the process for producing fiber preforms can yield materials not achievable from the melt, a new and large family of elements can be studied by NMR to determine the coordination, bondings, structural groupings, and other characteristics on an atomic scale that determine the microscopic characteristics of the fiber.

#### [ 5.] Polarization Maintaining Fibers

The impetus for creating polarization maintaining fibers comes from two different sources. Perhaps the most immediate of these is in optical fiber sensors in which deviations from a specific state of polarization may be associated with the presence of, for example, an electric or magnetic field. It is necessary for these fibers to maintain polarization in the absence of the external disturbance i.e., magnetic or electric field, which the sensors attempt to measure. A further need for high quality polarization maintaining fibers might be in some future coherent communications system.

Polarization preservation in fibers may be generically divided into two different types: low birefringence, and high birefringence. If we can envision a low birefringence single mode fiber that in some sense is "perfect" with regard to uniformity of dopant and uniformity of external influences on the fiber, then this ideal device will maintain its polarization. Unfortunately, there are a myriad number of internal as well as external influences that disturb this ideal depiction. Any physical imperfections in the fiber itself, as a consequence of lack of circularity from some quirk in the production process, or any micro-bubbles or cracks in the fiber will cause a random interaction between the two propagating modes of different polarization that are present in a single mode fiber, and the polarization maintaining characteristics of the fiber will be lost. In addition, any asymmetrical lateral stress, of either internal or external nature, bending, tension, torsion, and electric and magnetic fields, will also destroy polarization maintaining features. For example, a small axial scratch on the

surface of a drawn fiber produces a huge stress singularity if the fiber is subjected even to a slight twist. All of these effects influence the polarization coupling of the different modes that propagate in the fiber and degrade the ability of the fiber to maintain a single polarization.

Since low birefringence fibers can be affected in a number of ways by internal imperfections or external disturbances, we consider an alternate approach taken by other researchers, that is to increase the birefringence of the preform, and hence the fiber, through the deliberate introduction of a high degree of internal stress and azimuthal asymmetry in the fiber. It is upon this latter aspect that this research shall focus. This work will be carried out in cooperation with Prof. K.S. Kim, of the University of Illinois.

To insure that a high birefringence fiber has the capability of maintaining a specific state of polarization, it is necessary that some asymmetry in the azimuthal direction be included in the fiber. There are several ways in which this may be done. Japanese manufacturers, in particular Sumitomo and Hitachi, rely on an elliptical core within a circular cladding. Depending upon the cladding material and profile, the fast axis may be along either the semi-major or the semi-minor axis. Bell Laboratories has recently reported on the polarization preserving characteristics of a fiber pulled from a preform that had been flattened on two sides before being pulled. This seemed to have the advantage that the preferred axis could be located from the external shape of the pulled fiber. Another method, introduced by the group under Professor A. Gambling at the University of Southampton, England, attempts to make fuller use of the mechanics of stress induced birefringence in fibers in order to create the desired degree of azimuthal asymmetry. This is done by localized heating to remove dopants leaving an azimuthally asymmetric dopant profile in the preform. We plan to investigate multi-dimensional effects of stress birefringence in preforms and fibers. Our theoretical program will be complimented by experimental studies employing laser etching of dopants to achieve a highly controlled degree of azimuthal stress asymmetry in the preforms fabricated in our laboratory. Significant progress has already been made in optimizing stress distributions in fibers and preforms.

Zinc chloride, an extremely hygroscopic material, has the ability to form a low temperature glass. It transmits best in the mid infrared, and its infrared edge absorption allows transmission up to 10.6 microns. We are investigating the possibility of vapor phase deposition of this material via a suitable organic precursor, with subsequent removal of water by flowing HCl through our deposition system. A possible substrate tube would be polyvinylidene fluoride which is quite impervious to water. If this material is easily obtainable in rods or tubes, it could be used as a substrate in an MCVD process for obtaining dry, glassy zinc chloride that could result in a graded index preform (when doped with barium chloride).

#### [ 7.] Nonlinear Interactions in Glasses and Fibers

With the ability to dope fiber preforms with special elements, it is of interest to study non-linear effects in fibers. As a consequence of their small core diameters, it is possible to achieve non-linear effects in single mode fibers with modest laser powers. The two main thrusts which we would like to address are nonlinear frequency generation in optical fibers and nonlinear propagation and material damage in glasses and fibers. The first of these efforts will focus on understanding the behavior of the nonlinear second order susceptibility of glasses using tunable stimulated scattering in fibers with emphasis on coherent phonon contributions to the response. Secondly we will study the effects of explosive phonon build up on problems of laser induced damage in glasses. This effort will utilize self focusing effects and filament characteristics to study the problem.

##### [a.] Raman Amplification in Single Mode Fibers

The use of intense pump sources to generate gain at the sum and difference frequencies of the pump and a molecular resonance has been well studied. This effect has been shown to produce enormous gains at the lower Stokes frequency in liquid and solid media due to the high atomic densities available. Recently, several experiments have demonstrated that optical fibers are excellent candidates for generating Stokes gain and lasing at the down converted frequency. This is primarily due to two reasons: 1) fibers may support several tens of watts of pump power in extremely small cross sectional areas (20 microns<sup>2</sup>)

satisfying the requirement for large intensities required for nonlinear frequency generation, and 2) fibers may provide extremely long interaction lengths in a small volume.

Raman amplification has been demonstrated at 1.2 microns with a 1.06 micron pump by Koepf, et. al, and has generated a gain of  $10^3$  in 1 km with only 1.4 Watts of pump power. This experiment has defined the other physical mechanisms, such as Brillouin scattering effects, which limit the gain, allowing for a reasonable engineering design to achieve a given power output at the desired wavelength.

The recent development and characterization of Alexandrite lasers has resulted in a tunable intense source between 7000-8000 Å. The tunability and intensity will allow for the experimental probing of the molecular Raman scattering cross sections behavior in glasses by frequency resolved gain and pump measurements. The work will be aimed at understanding the effects of other coherent processes such as stimulated forward and backward Brillouin scattering on the stimulated Raman scattering (SRS) process. In particular, the quenching of phonon processes in glasses may be studied in this way by temperature dependent experiments on SRS gain.

#### [b.] Self Focusing and Laser Induced Damage

It is well known that materials which have positive Kerr nonlinearities result in self focusing and filament formation. The effect is due to the positive intensity dependent lens which results in a Kerr medium due to the peaked transverse intensity distribution of the propagating beam. This effect has resulted in light filaments less than 1 micron in diameter at visible wavelengths. This focusing results in damage in most materials, and the phenomenon is not understood. The primary problem lies in the fact that not enough power is absorbed to result in simple thermal damage. We would like to study the problem with a focus on non linear coherent generation of phonons at the self focusing catastrophe point. The generation rate of phonons has been shown to be unstable in SRS due to the boson behavior of the phonons. This approach to the damage problem could be studied in glasses with both amorphous and crystalline structure in order to assess the effects of coherently induced phonons in the optical damage problem. Needless to say, self focusing of this magnitude could play an important role in coupling into fibers for energy transfer.

#### [ 8.] "Smart Skin" Materials with Embedded Fiber Sensors

As increased demands are placed upon the development of composite materials to be employed near the limits of new technologies, it becomes necessary to monitor their state with regard to temperature and strain in a continuous manner. A technique that holds promise of fulfilling this goal is that of embedding optical fiber sensors in the material as it is being processed. These fibers must be able to operate over the same range of temperature and strain as the host composite. By measuring the light passing through the fiber, it is possible to determine information on the state of the surrounding composite.

Thus far, with few exceptions fibers, have been designed primarily for telecommunication, and, in spite of the rapidly growing sensor market, not sufficient effort has been expended to optimize the fiber design for its specific sensing role. This question must be addressed if there is to be any hope of embedded fibers fulfilling their promise. As noted above, Brown is one of the very few universities capable of designing and fabricating all stages of state-of-the-art optical fibers. Fiber design with respect to novel dopants that can maximize the sensitivity to temperature and strain will be one emphasis of our program. It has been noted that certain rare earth elements, in particular Nd, exhibit a marked temperature sensitivity, and we will study the effects of dopant levels upon temperature sensitivity for embedded fibers. Since we will limit ourselves to consider maximum lengths of fiber of the order of a hundred meters or so, attenuation due to higher dopant levels will not be a limiting factor as would be in the case of the design of a telecommunications fiber.

One of the techniques used in the interrogation of a specific fiber section is that of OTDR (Optical Time Domain Reflectometer). In this technique, an optical signal of short duration is launched into an optical fiber. At each point in the fiber, there is some amount of backscatter from this pulse. The amount of backscatter is dependent upon the fiber design, both geometry, the material with which the fiber is doped, the level of doping, and the the local state of temperature and stress. Clearly this is a system with many parameters. Knowing the speed of propagation of the wave in the fiber, and knowing the time difference between the introduction of the pulse into the fiber and the time of the return of the back scattered wave, it is possible to obtain information on the local position from which the pulse was scattered. This back scattered pulse can provide information on temperature, strain, and other characteristics of the fiber locally. One of the

problems associated with such a technique is that the speed of light travels approximately 30 cm/nsec, and thus, if we wish a resolution (spatially) of 1 cm, we must have a shutter system that can open and close in  $1/30$  of a nsec. It is possible to introduce splices, or discontinuities in the fiber that increase backscatter, and if their location is known, they can increase the spatial resolution for this technique. However, splicing of fibers over a length of many meters, or even tens or hundreds of meters, is not a practical solution to the problem of enhancing backscatter or increasing spacial resolution.

We propose the following technique, which is simple to implement in an on line manner on an optical fiber draw tower. It is well known that radiation can induce structural defects in glass that can enhance scattering. We consider a laser mounted on a draw tower, pulsing at regular intervals to intersect the prior to coating. The intensity could be varied, or the pattern of radiation induced defects could be changed, depending upon the laser pulse shape and duration. Thus, the reflected signal would be associated with a specific region of the fiber that, in conjunction with standard OTDR techniques, could markedly increase spatial resolution.

This work is to be carried out with Prof. K.S. Kim, of the Theoretical and Applied Mechanics Group at the University of Illinois, Urbana, Ill., and with Prof. J. Cornie, of the M.I.T. Laboratory for the Characterization of Composite Materials.

#### [ 9.] MCVD Deposition for Gradient Index Lenses

Supported by the Army Research Office, Durham, N.C., \$300,000, 36 months. Within recent years there has been increasing interest in the use of gradient index lenses in numerous optical situations. In such a device, either a radial, or axial (or both) variation in the index of refraction causes the light passing through it to be bent. The classic example is the Wood lens in which there is a radial variation in the index of refraction. Depending on the index profile, a flat lens of this design can serve either as a converging or diverging lens. Another configuration of the same genre is the optical fiber preform, with which our laboratory has had much experience. Although perhaps not strictly classified as a gradient index lens, the optical fiber is a classic example of how structured gradients can channel light to achieve low loss transmission of information at a density that would have been inconceivable a decade ago. New technologies have been developed to insure the extremely

tight tolerances on geometry and impurity levels. In all of these techniques, the goal is to structure a preform rod of extremely high purity, with a radial (or, in the case of polarizing maintaining fibers, azimuthal) distribution of dopants that will insure that the incoming light will be confined within the fiber. Much of the behavior of such fibers can be described with conventional ray optics, and, driven by commercial incentives, the work in this area in our leading industrial laboratories has been extensive.

In this proposed research, we wish to employ the techniques of optical fiber preform fabrication, in particular MCVD (Modified Chemical Vapor Deposition, to be described below) to the fabrication of preform rods that could serve as radially structured gradient index lenses. In the development of preforms for optical fibers, the chief design criterion is the need for ultra-high purity to insure that fiber pulled from the preform will have low losses, of the order of a few Db/km. For a radially structured preform rod to be used as a gradient index lens (i.e., the preform rod is sliced to produce many lenses), the stringent requirements on low absorption may be relaxed; however, a more carefully structured index of refraction (as a function of radius) is required. This gives us the freedom to consider a host of glasses that have traditionally been used as optical elements but whose absorption renders them unsuitable for use in optical fibers. Prof. D. Moore, of the University of Rochester Institute of Optics, has worked extensively in this field over the past years, and we have been in close contact with him in structuring the goals of this proposals.

### **Equipment and Facilities**

As noted above, there are three components of our laboratory: 1). an MCVD (Modified Chemical Vapor Deposition) Laboratory in which vapor phase techniques are employed to fabricate silica based preforms designed in our laboratory, 2). a fiber characterization laboratory containing a York Technology Preform Analyzer the provides a three dimensional profile of the index of refraction of our preforms, and a York Technology FCM 1000 Fiber Characterization Station (a donation from the Bell Communications Research, and 3.) a complete optical fiber draw facility. This equipment was purchased from Special Gas Controls and is an eight meter draw tower with a 25,000 W carbon resistance furnace, two ultraviolet cured coating stages, and the possibility of a thermally cured silicone coating stage. There are three Beta gauges, one for feedback and one for for fiber diameter control.

and two coating diameter monitors. The tower has been operational since August 1987. Our first fiber (a phosphorus-germanium core fiber to study second harmonic generation) was drawn to  $125\ \mu$  with a tolerance of  $\pm 0.2\ \mu$ .

A Micro-Vax II has been installed on an Ethernet link to a series of larger Digital Equipment machines and will be used to control and coordinate some of our laboratory activities. In addition, we have two Model 41C Coherent Radiation carbon dioxide industrial lasers. The output is approximately 270 W. One laser was a gift of the IBM Corporation to our laboratory, and the other was donated by the Florsheim Shoe Company of Chicago, Ill. We also have a smaller "home built" carbon dioxide laser, and a pulsed 1 J carbon dioxide TEA laser. Further, there are two fume hoods, including a floor "walk in" model. Other equipment in this laboratory consists of oscilloscopes, detectors, pumps, He-Ne lasers, and an optical table. There is also a full machine shop available for any work that might need to be done in the construction of equipment.

In addition to the equipment cited above in our laboratory, the laboratories of Prof. Risen (Chemistry) and Bray (Physics) contain considerable equipment used for glass research. These include NMR spectrometers used primarily for  $^7\text{Li}$ ,  $^{11}\text{B}$ ,  $^{17}\text{O}$ , and  $^{19}\text{F}$ . A new FTNMR will be truly multinuclear, of great importance for the rare earth elements we wish to consider. (Prof. Bray). In the laboratory of Prof. Risen, there is a new Spex Ramalog MicroRaman spectrometer with Spectra Physics 4 W (all lines)  $\text{Ar}^+$  laser. The Microraman has a spatial resolution of 2 microns. In the infrared and far-infrared there is a Digilab FTS15B Fourier Transform Infrared Spectrometer that can take relatively good spectra between  $50\text{-}4000\ \text{cm}^{-1}$ . In addition, the Optical Facility has purchased a BOMEM DA3.1 FTIR with its initial configuration having a range of  $30\text{-}40,000\ \text{cm}^{-1}$  as well as microscopic infrared capabilities. There are a number of high temperature furnaces, the most advanced of which is a CM Rapid Temp 1700B Furnace with a sustained temperature to  $1600\ ^\circ\text{C}$ . In addition, there are also extensive facilities available for the measurement of fast optical processes, electron microscopes, ion microprobes, as well as a complete microelectronics laboratory for vapor deposition and encapsulation. This latter equipment may play a role in future structuring of devices on fibers.

Our present equipment provides a natural complement to the extensive bulk characterization facilities for the physical properties of glasses. We will be able to analyze our

preforms with a sophisticated FTNMR. This will be particularly important for studies in which we wish to determine the manner in which dopants are incorporated into vapor phase deposited preforms. Further, a micro Raman probe in the laboratory of Prof. Risen of the Chemistry Department will enable us to scan preforms and fibers with a a high degree of spatial resolution. This equipment will prove of great value in detailed characterization of the preforms and fiber samples that are produced in our laboratory. We will be able to produce new glass structures and compositions not attainable with crucible techniques.

END  
DATE  
FILMED  
5-88  
DTIC